

# Enhancing NOMA performance in uplink MMW-RoF mobile fronthaul systems by using index modulation

Shen-Chen Tsai<sup>1</sup>, Jhih-Heng Yan<sup>2</sup>, Kai-Ming Feng<sup>1\*</sup>

<sup>1</sup> Institute of Communications Engineering, National Tsing Hua University, Hsinchu City 30013, Taiwan

<sup>2</sup> Chunghwa Telecom Co. Ltd., Taoyuan City 32661, Taiwan

\*kmfeng@ee.nthu.edu.tw

**Abstract:** A novel OFDM-based index modulation (IM) assisted multi-users NOMA wireless uplink system is demonstrated in MMW-RoF mobile fronthaul. With IM, the proposed scheme achieves higher flexibility on spectral efficiency and power ratio than conventional NOMA.

## 1. Introduction

To meet the exponentially growing capacity demands in modern mobile communication systems, increasing transmission data rate has always been the major challenge. In current 5G mobile networks, the vast available spectrum in millimeter wave (mmW) regime will be employed to relieve the spectrum scarcity in sub-6 GHz microwave frequency range [1]. Meanwhile, non-orthogonal multiple access (NOMA) is a promising technique to increase system throughput to allow multiple users to share the same time and frequency resources [2]. Therefore, combining mmW and NOMA technologies is potentially considered as a key player in boosting 5G network capacity and next generation radio access networks. In classic power domain NOMA scheme, to well distinguish different users' signals, the power ratio between any two users has to be kept at a fix number for best NOMA demodulation with successive interference cancellation (SIC) process. As an example, the power ratio between two 4-QAM signals usually is optimized at 6-dB to get the best performance [3]. However, such an optimal power ratio is hard to be maintained, especially in the uplink radio access networks. As shown in Fig. 1, users served by one remoted radio unit (RRU) may have different channel qualities: good line-of-sight links (CH1); edge users with low channel gain due to high mmW path loss (CH2); and/or users with severe link degradations due to channel blockage or antenna beam pattern misalignment (CH3). Such channel variations may not be able to retain a suitable received power ratio among users at the RRU and will eventually degrade system performance.

In this paper, we take the advantages of OFDM with index modulation (OFDM-IM) technique [4, 5] to provide a flexible system design to balance the system's error performance and spectral efficiency. We employ the proposed OFDM-IM modulation scheme to the "low-power" signal in a power domain NOMA (NOMA-IM) scheme to improve the overall performance. Our experimental results not only validate its feasibility and power-ratio flexibility of the NOMA-IM, but also demonstrate that NOMA-IM has the ability to mitigate multi-user interference by adjusting IM parameters.

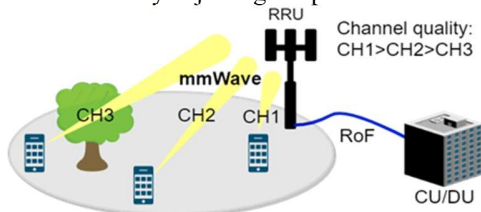


Fig. 1 Schematic diagram of an uplink MMW-RoF system with different wireless channel qualities

TABLE I  
LOOK-UP TABLE FOR  $N=4$  WITH DIFFERENCE  $K$

N=4, K=3			N=4, K=2			N=4, K=1		
Bits	Index	Sub-blocks	Bits	Index	Sub-blocks	Bits	Index	Sub-blocks
[0, 0]	1	[0, s, s, s]	[0, 0]	1	[s, 0, 0, s] ([0, s, 0, s])	[0, 0]	1	[s, 0, 0, 0]
[0, 1]	2	[s, 0, s, s]	[0, 1]	2	[s, s, 0, 0]	[0, 1]	2	[0, s, 0, 0]
[1, 0]	3	[s, s, 0, s]	[1, 0]	3	[0, 0, s, s]	[1, 0]	3	[0, 0, s, 0]
[1, 1]	4	[s, s, s, 0]	[1, 1]	4	[0, s, s, 0] ([s, 0, s, 0])	[1, 1]	4	[0, 0, 0, s]

## 2. Operation of the proposed NOMA-IM

The index modulation applies the operation status of the resources, such as frequency subcarriers and time slots, as the index values to embed extra information in the communication system. In this work, taking the inherent nature of OFDM, we can embed extra bits by turning ON or OFF the frequency subcarriers as the index values for our OFDM-IM. At the receiver, the active/silent subcarrier combinations are identified to recover the extra information embedded by IM. As an example, Table I illustrates a look-up table for  $N = 4$  case, i.e., 4 subcarriers per sub-block, that will be applied in our experiment. In Table I, there are three different  $(N, K)$  combinations, including 3, 2, and 1 active subcarriers ( $K$ ) out of 4 in each sub-block, which are represented as  $(N4, K3)$ ,  $(N4, K2)$ , and  $(N4, K1)$ , respectively. We can see that there exists only one one-to-one mapping for  $(N4, K3)$  and  $(N4, K1)$ , therefore, there's no redundant state existed. However, when  $K = 2$ , the number of subcarrier combinations  $C_2^4 = 6$  is not a power of 2, thus there exist two combinations, i.e.,  $([0, s, 0, s])$  and  $([s, 0, s, 0])$  in Table I, that are not used at the transmitter. At

the receiver, these unemployed combinations may still appear after active/silent subcarriers identification process due to noise or channel interferences. In such cases, following the shortest Hamming distance, we enforce the unemployed combinations into suitable bit combinations at the receiver's look-up table for  $K = 2$ .

In wireless uplink networks, the RRU typically receives higher power from the near users and limited power from the far users due to high mmW path loss and/or channel blockage. In our proposed NOMA-IM uplink wireless access system, we combine one conventional OFDM signal for the near user (strong) and another OFDM-IM signal for the far user (weak) in a power domain NOMA scheme. When two conventional 4-QAM OFDM-NOMA signals simultaneously arrive at the receiving antenna of the RRU, the power ratio between these two signals usually needs to be kept at 4:1 to achieve the best BER performances [3]. Therefore, as shown in Fig. 2(a), the optimal Euclidean distance (ED) ratio between the origin point and the 4-QAM constellation points of these two users is kept at 2:1 and the overlapped constellation looks like a 16-QAM signal. For the OFDM-IM (far user), since some subcarriers are silent, the cumulated constellation will have one extra symbol at the origin. Thus the overlapped constellation of the proposed NOMA-IM will be obtained as seen in Fig. 2(b). In this case, the ED ratio can be still upheld at 2:1 by adjusting the IM parameters, even under different power ratios. As an example, let the power of conventional ( $N_4, K_4$ ) OFDM signal be  $P_s$ . Based on the same ED in the symbols, the power of ( $N_4, K_3$ ), ( $N_4, K_2$ ), and ( $N_4, K_1$ ) OFDM-IM signals will be  $3P_s/4$ ,  $2P_s/4$  and  $P_s/4$ , respectively. Thus, the power ratio between OFDM ( $P_H$  for near user) and OFDM-IM ( $P_L$  for far user) is determined by the number of  $K$  with the same ED ratio. Hence, if the ED ratio  $\sqrt{P_H} : \sqrt{P_L} = 2:1$ , the corresponding power ratio  $P_H : P_L$  of ( $N_4, K_3$ ), ( $N_4, K_2$ ) and ( $N_4, K_1$ ) will be 16:3 (~5:1), 16:2 (8:1) and 16:1 in the proposed NOMA-IM, respectively.

### 3. Experimental setup and results

The experimental setup of the uplink mmW RoF mobile fronthaul system is depicted in Fig. 3. At the transmitter, both signals' FFT sizes are 1024, in which 60 of them carry information. For the near user, 4-QAM are encoded on all the 60 subcarriers, while the far user's signal are modulated with 4-QAM along with the proposed IM scheme. In the IM scheme, 60 information bearing subcarriers are divided into 15 sub-blocks, i.e., 4 subcarriers in each sub-block. Then, the two signals go through the same OFDM signal processing with a cyclic prefix of 1/8 and then are fed into an arbitrary waveform generator (AWG) with 12 GS/s to generate the corresponding OFDM (near user) and OFDM-IM (far user) signals at an intermediate frequency (IF) of 4 GHz and the total signal bandwidth of each user is 810 MHz. The two IF signals are next up-converted to 29 GHz mmW frequency, amplified by power amplifiers (PA), and then transmitted by two 23dBi horn antennas, spaced by 1.5 m.

After ~1.5-meter wireless transmission from the two users to RRU, the far user's power is manipulated by adjusting the antenna's output power to emulate different channel qualities. As the single horn antenna at the RRU detects both signals from the two users, the received superposed NOMA-IM signal is amplified by a low noise amplifier (LNA) and down converted to 9 GHz by a mixer. The down converted signal is then converted to optical domain by a 10 GHz Mach Zehnder modulator (MZM) at 1550 nm to generate the RoF up-stream signal in the mobile fronthaul system. After 15-km single mode fiber (SMF) transmission, the RoF signal is detected by a 10 GHz photodetector (PD), and then input to an 80 GS/s real time scope (RTS) to capture signal waveforms for the following offline digital signal processing.

The offline digital signal processing has two stages. In the first stage, we hard-decide the near user's (strong) signal from the received NOMA-IM signal via conventional OFDM-NOMA demodulation processes. In the second stage, we follow the conventional SIC process to reconstruct the far user's (weak) waveform, and then demodulate the far user signal by either OFDM or OFDM-IM demodulation process, majorly by looking up with Table I, and calculate the BER for performance comparison.

Figure 4 summarizes all the BER curves as a function of received optical power (ROP) to quantify the transmission quality of the overall link for all scenarios. For a fair comparison, in each NOMA-IM case, we set the

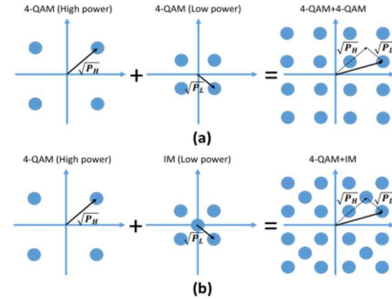


Fig. 2 Combined constellation of (a) NOMA, and (b) NOMA-IM

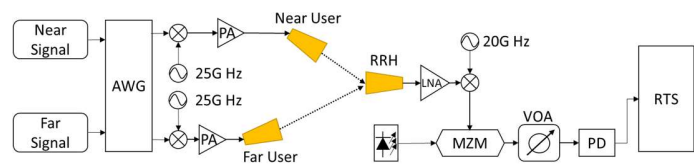


Fig. 3 Experimental setup

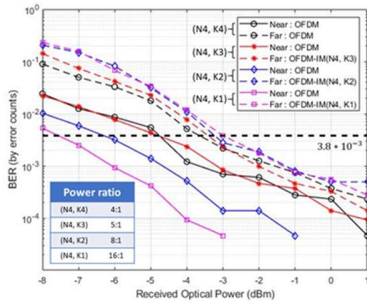


Fig. 4 BER curves with fixed power ratio.

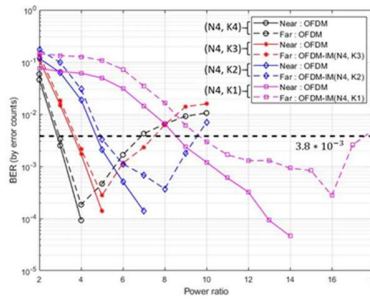


Fig. 5 Power ratio versus BER with different combinations

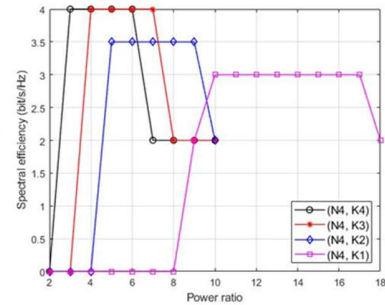


Fig. 6 Spectral efficiency versus Power ratio with different combinations

ED ratio between the two users at 2:1, same as the optimized setting for conventional NOMA. Thus, the power ratios between the two users are respectively 4:1, 16:3 (~5:1), 8:1 and 16:1 for  $(N4, K4)$ ,  $(N4, K3)$ ,  $(N4, K2)$  and  $(N4, K1)$ , where  $(N4, K4)$  denotes conventional OFDM-NOMA signals without IM. We can see that the BER values of the far user (dash lines) only slightly degrade as  $K$  decreases because the ED and each subcarrier power for far user are kept the same for all the active subcarriers and less interference is induced from the near user under NOMA-IM scheme. In contrast, the near user's performance (solid lines) is greatly enhanced as  $K$  decreases. This is because, as  $K$  decreases, i.e., less active subcarriers in the far user's signal, not only the shared optical power for each subcarrier of the near user is increased, but the overall interferences from the far user's signal become less. Therefore, it demonstrates that the NOMA-IM has the ability to mitigate multi-user interference by adjusting the parameter of  $K$ .

We evaluate the BER performance with different power ratio between the two users with 4-QAM signal format for different  $(N, K)$  combinations in Fig. 5, thus the ED ratio between the two users is no longer fixed. In this measurement, the ROP is fixed at 0.5 dBm after 15 km SMF transmission. For classic  $(N4, K4)$  NOMA scheme, the best BER performance occurs at 4:1 power ratio between the two users, as expected. Further increasing power ratio can further enhance the near user performance, but degrade the far user's signal integrity due to less shared power. To meet the FEC threshold for the far user, the power ratio can be ranged from 3:1 to 6:1, as shown by the black dashed line in Fig. 5. When  $(N4, K3)$  is employed, the best operation power ratio is about 5:1 and the power ratio range that can guarantee the far user to meet FEC criterion is from about 4:1 to 7:1. For  $(N4, K2)$  and  $(N4, K1)$ , same as expect, the best power ratios are 8:1 and 16:1 and the power ratio ranges to satisfy FEC limit for far user are from 5:1 to 9:1 and 10:1 to 17:1, respectively. Thus we can see that the power ratio operation ranges for the far user are greatly relieved by using the proposed NOMA-IM scheme.

In Fig. 6, we calculate the usable spectral efficiency under different power ratio when both the users' BERs meet the FEC threshold in each combination. It can be found that the allowable operating power ratio range for conventional power domain NOMA is strictly limited, although it can reach the highest spectral efficiency in this range. However, when the power ratio exceeds 6:1, the far user's signal fail to meet the FEC limit, thus the spectral efficiency is dropped by half and the system can only serve for the near user. For the proposed  $(N4, K3)$  NOMA-IM scheme, it can also achieve the same spectral efficiency as conventional NOMA. When adjusting the IM parameter to  $(N4, K2)$ , the near and far users can respectively receive a maximum spectral efficiency of 2 and 1.5 bit/s/Hz (4 bits from active subcarriers and 2 bits from IM) for the power ratio beyond 6:1. Thus the combined spectral efficiency is 3.5 bit/s/Hz for power ratio ranged from 5 to 9. Moreover, the bearable operation power ratio can be extended from 10 to 17 for  $(N4, K1)$ , which means, even at 17:1 power ratio, the far user can still receive a spectral efficiency of 1 bit/s/Hz: 2 bits from the single active subcarrier and 2 bits from IM. Thus, the composite spectral efficiency for the two users can still be 3 bits/s/Hz. Hence, if the power budget is greatly lost for the far user, the proposed NOVA-IM can greatly relieve the multi-user's multiplexing criteria in the power domain by adjusting IM parameters in higher power ratio scenarios where conventional NOMA cannot normally operate. Thus, NOMA-IM can be easily adapted to satisfy different channel quality owing to the index modulation characteristics.

#### 4. Conclusions

We propose a power domain NOMA scheme with OFDM-IM modulation. The experimental demonstrations, with a 2-by-1 mmW uplink setup, show that the power ratios can be ranged from 4:1 to 17:1, which significantly enhances the feasibility of mmW NOMA in various challenging transmission environment.

#### 5. References

- [1] T. S. Rappaport *et al.*, *IEEE Access* **1**, pp. 335-349, 2013.
- [2] Y. Saito, *et al.*, doi: 10.1109/VTCSpring.2013.6692652.
- [3] S. Shen, *et al.*, *OFC 2020*, paper M2F.3.
- [4] E. Basar, *et al.* *IEEE Access* **5**, pp. 16693-16746, 2017.
- [5] T. Tang, *et al.* *JLT* **36**, pp. 4501-4506, 2018.